Feasibility of Ultraviolet Light Emitting Diodes as an Alternative Light Source for Photocatalysis

Lanfang H. Levine and Jeffrey T. Richards
Dynamac Corporation, Kennedy Space Center, FL

Robert Soler and Fred Maxik
Lighting Science Group Corporation, Satellite Beach, FL

Janelle Coutts
Department of Chemistry, University of Central Florida, Orlando, FL

Raymond M. Wheeler
Engineering Directorate (NE-S), Kennedy Space Center, FL

ABSTRACT

The objective of this study was to determine whether ultraviolet light emitting diodes (UV-LEDs) could serve as an alternative photon source efficiently for heterogeneous photocatalytic oxidation (PCO). An LED module consisting of 12 high-power UV-A LEDs was designed to be interchangeable with a UV-A fluorescent black light blue (BLB) lamp in a Silica-Titania Composite (STC) packed bed annular reactor. Lighting and thermal properties were characterized to assess the uniformity and total irradiant output. A forward current of (I_F) 100 mA delivered an average irradiance of 4.0 mW cm^{-2}, which is equivalent to the maximum output of the BLB, but the irradiance of the LED module was less uniform than that of the BLB. The LED- and BLB-reactors were tested for the oxidization of 50 ppm_v ethanol in a continuous flow-through mode with 0.94 sec space time. At the same irradiance, the UV-A LED reactor resulted in a lower PCO rate constant than the UV-A BLB reactor (19.8 vs. 28.6 nM CO_2 sec^{-1}), and consequently lower ethanol removal (80% vs. 91%) and mineralization efficiency (28% vs. 44%). Ethanol mineralization increased in direct proportion to the irradiance at the catalyst surface. This result suggests that reduced ethanol mineralization in the LED-reactor could be traced to uneven irradiance over the photocatalyst, leaving a portion of

the catalyst was under-irradiated. The potential of UV-A LEDs may be fully realized by optimizing the light distribution over the catalyst and utilizing their instantaneous "on" and "off" feature for periodic irradiation. Nevertheless, the current UV-A LED module had the same wall plug efficiency (WPE) of 13% as that of the UV-A BLB. These results demonstrated that UV-A LEDs are a viable photon source both in terms of WPE and PCO efficiency.

IMPLICATIONS

Hg-vapor lamps are common UV sources for photocatalysis but create safety and environmental concerns because they contain Hg; furthermore they have a relatively short life span. This paper demonstrated that the UV-A LED is a viable alternative to the Hg-vapor lamps without sacrificing PCO efficiency if the design of the LED arrays is improved to increase the irradiant uniformity. The use of LEDs could eliminate hazardous Hg wastes and extend photocatalysis application to places requiring more compact and robust air purification solutions.

INTRODUCTION

The ability of titanium dioxide (TiO_2)-assisted photocatalytic oxidation (PCO) to decompose (mineralize) a broad range of organic contaminants into CO_2 and H_2O at room temperature has attracted attention for various environmental applications. This technique has been investigated as an alternative or complimentary method for air contaminant control[1-7] as well as a means for treating water and wastewater.[7] The TiO_2-catalyzed PCO process typically requires a light source with a wavelength less than 388 nm. Mercury vapor lamps such as UV-A black lights and UV-C germicidal lamps have been widely used in laboratory and commercial PCO systems (e.g. GENESIS AIR PHOTOCATALYST GAP™, Ultra Sun Technologies, and Mazyck Technologies). But these lamps contain trace amounts of toxic mercury, there are fragile, and have a relatively short life span (<12,000 hrs). Mercury is a highly toxic and controlled substance, and it is increasingly becoming controlled or banned by government safety and environmental regulators. Although there are non-mercury lamps, e.g., microwave generated UV sources, the lamps are driven by magnetrons that must withstand long duty cycles and the microwaves must be contained for safety purpose.

On the other hand, light emitting diodes (LEDs, semiconductor-based lighting devices) are compact, reliable, and long lasting devices. LEDs are driven by direct current, can accommodate faster switching, and do not contain toxic Hg. They are entering the market of various illumination applications with an unprecedented speed. Since the development of first commercial visible LEDs in 1968, the light output from a single device has increased by a factor of 20 per decade, while the price in US dollar per lumen has declined by a factor of 10 per decade.[8] White-light LEDs are now surpassing the efficiency of linear fluorescent and compact fluorescent lamps.[8] Ultraviolet light emitting diodes (UV-LEDs) have been commercially available since 2003. Currently, UV-A LEDs have a life expectancy of 50,000 hrs at L50, about 5 times that of Hg-vapor lamps. Naturally they have been considered as an alternative light source for photocatalysis for both gaseous[9,10] and aqueous applications.[11,12] However, most of the PCO-studies to date were conducted with low-power LEDs of varied wavelengths including those outside of the TiO_2 action spectrum (e.g. 395 and 405 nm [11,12]) in different reactors. Chen et al. studied photocatalytic degradation of percholoroethylene (PCE) in a rectangular steel gas-phase reactor irradiated by 375 nm UV LEDs (16 Nichia LEDs with 1.0 mW power output) and found only 43% degradation of PCE in the LED reactor, while there was 90% degradation in a UV-A black light reactor.[9] This result seemed to imply that LEDs are less effective than the black light. Ciambelli et al. investigated the photocatalytic breakdown of benzene in a lab scale fluidized bed reactor irradiated by two or four UV (365-nm) LED modules (Nichia Corporation) and showed a 27% conversion of benzene into CO_2 at 80 °C.[10] Although these studies proved that UV LEDs have promise as a light source, no data were provided regarding their PCO performance relative to mercury-vapor lamps at the same irradiance, their actual power use efficiency, or issues related to the LED integration into PCO reactors. The objective of this study was to design an LED PCO reactor and compare the performance of state-of-the art UV-A LEDs to that of a Hg-vapor UV-A fluorescent black light for low temperature PCO degradation of organic contaminants.

EXPERIMENTAL METHODS

Light Sources

An 8-W UV-A (F8T5) fluorescent black light blue (BLB) lamp from Philips was used as the control light source. The BLB lamp dimensions were 15.6 mm D x 304.8 mm L and the irradiant

output was 2.5 mW cm^{-2} at a 25.4 mm distance. The LEDs used for the study were high-power chip-type UV-A LEDs (model NCSU033B) from Nichia Corporation, having a peak wavelength of 365 nm, a spectrum half-width of 9 nm, and irradiance angle of 120 degrees. The optical output of a single LED was 325 mW at a forward current of 500 mA and voltage of 3.8 V (i.e., 1.9 Watts).

To conduct direct comparison of PCO efficiency with UV-A BLB, the LED source was designed based on three criteria: 1) interchangeability with the BLB in the same PCO reactor; 2) similarity of irradiance profile between the LED module and the BLB (i.e. isotropic); and 3) a wide range of irradiances, including one equivalent to that of the 8-W BLB. Based on this, we designed an LED assembly to simulate the geometry of the linear fluorescent bulb. The placement of individual LEDs was determined by modeling (Figure 1). Uniformity of the irradiance increased as the distance between LEDs decreased (Figure 1a). Thus an assembly with densely populated LEDs (e.g., 15 mm vs. 30 mm spacing between LEDs) would provide more uniform irradiance, but the power consumption and initial investment (number of the LEDs) would increase accordingly. In addition, greater numbers of LEDs create thermal management challenge, where lower operating temperatures are preferred to maintain the long operating life of the LEDs. The coefficient of temperature increase per unit electric power input is dependent upon the thermal resistance of the LED system (e.g., R_{ja} = 35 °C/W with Nichia's standard circuit board), density of the LED placement, and factors such as ambient temperature. The radial irradiance profile of the LED assembly was modeled based on four linear LED arrays evenly placed every 90-degrees in a 360-degree arrangement. The model examined the effect of viewing angle and distance between the light source and the object to be irradiated (Figure 1b). Since the object to be irradiated was the photocatalyst packed in an annular reactor (see details in PCO reactor design), optimal diameter (Ø) of the quartz sleeve separating the light source and the catalyst was subsequently determined by this modeling exercise. Although increasing the diameter enhanced the uniformity of light distribution, the radiant flux per unit area (E) decreased approximately following an inverse-square law (Figure 1b). Figure 1 suggests that 20-mm spaces between LEDs, and a 25-mm diameter would give satisfactory uniformity and sufficient intensity. Consequently, twelve LEDs were mounted on a 15.6-mm diameter aluminum rod in four linear arrays, three LEDs in each array with a space of 20 mm between the LEDs as shown in Figure 2.

Figure 1 and Figure 2 here

Photocatalytic Oxidation (PCO) Reactor

Silica-Titania Composite (STC) pellets (2 x 6 mm) from Sol-gel Solutions, LLC (Gainesville, FL) served as the photocatalyst. The STC has the same porosity (30 - 40 Å) and TiO_2 loading (4 g Degussa P-25 in 100 mL silica precursor, tetraethyl orthosilicate) as that used by Stokke and Mazyck.[13] An annular reactor shown in Figure 2 was used to carry out this study because of its simplicity and efficiency in utilizing traditional linear fluorescent lamps. It consisted of two concentric cylinders, with an annulus formed between an aluminum housing and a quartz sleeve. The light source was inserted in the middle of the quartz sleeve, while STC pellets were packed in the annulus. Two design parameters were optimized: 1) the diameter of quartz sleeve that determines the distance between the photocatalyst and light sources; and 2) the annulus size. The former was especially critical with LEDs as the light source. The effect of the quartz sleeve's diameter was illustrated in Figure 1b. The annulus space that determines the thickness of the catalyst bed should be small enough to ensure that photons emitted from the light source reach all catalyst surfaces uniformly and large enough to allow reproducible packing of STC pellets. Results of a preliminary light transmittance measurement showed that STC pellets in an annulus of 8 mm used by Stokke and Mazyck[13] attenuated 97% of a UV-A BLB light. This suggested the annulus size of the reactor should be further reduced. Key parameters of the bench-scale test reactor used in this study and that used by Stokke and Mazyck[13] are listed in Table 1 for comparison.

Table 1 here

Light Source Characterization

Spectral quality and quantity of the light sources were assessed to determine an optimal UV-A BLB for the study and the driving current required for the LED assembly to achieve an equivalent irradiance. Measurements were conducted outside the PCO reactor in a dark room using a spectroradiometer (OL754C, Optronics Laboratories, Orlando, FL). The light source (either BLB or LED assembly) was centered inside a quartz sleeve of the same dimension as that used in the reactor (Table 1) without the catalyst around it and placed directly above the

integrating sphere of the spectroradiometer. A light attenuation aperture of 12.7-mm in diameter was placed before the integrating sphere that has an opening of 31.8 mm in diameter. This setup (Figure 3) measured the irradiance immediately at the surface of the catalyst bed. For the LED module, measurements were taken every 5 mm along the lateral direction both directly opposite to one of four LED arrays (designated as angle 0 degree) as shown in Figure 3 and between two linear LED arrays (designated as angle 45 degree). Irradiant output of the LED assembly and LED die's temperature were measured at a range of forward current between 30-500 mA. The BLB was measured at three positions along the axis of the lamp.

Figure 3 here

PCO Tests

Performance of the UV-A BLB- and the LED-irradiated annular reactors was evaluated for oxidation of ethanol in an experimental setup (Figure 4) that allowed precise control of experiment variables and continuous monitoring of the PCO reaction. The setup consisted of: 1) a Kin-Tek air generator (model 491M, La Marque, TX) for supplying a simulated contaminant air containing 50 ppm_v ethanol (EtOH) and 72% relative humidity at 25 °C; 2) a PCO reactor packed with 14.6 g of STC pellets to a bed height of 60 mm; 3) two mass flow controllers for controlling the flows to the PCO reactor and CO_2 analyzer; 4) temperature sensors for the reactor's inlet and outlet as well as for room temperature; 5) humidity sensors for the reactor's influent and effluent air; 6) a CO_2 analyzer for the reactor effluent; 7) a sample stream selecting valve; and 8) a gas chromatograph (ThermoFinnigan, Austin, TX) equipped with a flame ionization detector (GC/FID) and a HP Plot Q capillary column (30 m x 0.32 mm, 20 μm depth of film).

Figure 4 here

All tests were carried out in a flow-through mode with an uninterrupted 2 L min^{-1} air flow containing 50 ppm_v EtOH under continuous illumination. Each test was repeated three times. Both influent and effluent were sampled alternately every 8.45 min and analyzed for ethanol and any oxidation intermediates by GC/FID. The effluent was also directed to a CO_2 analyzer to determine the production of CO_2, the complete mineralization product. CO_2 concentration was

recorded every minute. The reactor was maintained at 25 °C via forced air convection using a heat sink attached to the PCO reactor. The STC pellets were pre-conditioned with 72% RH, VOC-free air under continuous illumination. Each test began with the addition of ethanol to the air stream and continued for 21 hours, followed by regeneration with humidified, VOC-free air and continuous illumination. The same batch of STC catalyst was used for all runs. Completion of the regeneration was indicated by no detectable organic species and only baseline-level CO_2 in the effluent.

PCO Efficiency, Kinetics and Photonic Efficiency

PCO performance was quantified in terms of EtOH removal and mineralization efficiency (X_A). The former is a measure of the total removal of the test VOC, whether it is removed by adsorption or oxidation, while the latter is a measure of the complete oxidation of EtOH to CO_2. These values were calculated using equations 1 and 2, respectively. C_0 and C_{EtOH} are the influent and effluent EtOH concentrations, and $\Delta C_{carbon\ dioxide}$ is the CO_2 generated from the PCO process. The rate of photocatalytic oxidation of ethanol was determined based on the formation of CO_2 instead of the disappearance of ethanol to prevent overestimation due to the adsorption of EtOH to the photocatalyst. Cumulative CO_2 concentration was plotted against time, a linear relationship between the concentration and time suggested zero-order kinetics. The slope gave rise to the PCO rate (r). PCO photonic efficiency (ξ) was calculated as the ratio of the photocatalytic degradation rate to the incident photon flux (eq 3).

$$\text{EtOH removal} = (C_0 - C_{EtOH})/C_0 \quad (1)$$

$$X_A = \Delta C_{carbon\ dioxide}/2 \times C_0 \quad (2)$$

$$\xi = \text{Rate of reaction (M sec}^{-1}\text{)/rate of photon incident (mol sec}^{-1}\text{)} \quad (3)$$

RESULTS AND DISCUSSION

Spectral Quality and Quantity of the Light Sources

Photon flux, or irradiance, on the catalyst surface is one of the most important factors affecting photocatalytic oxidation efficiency. The LED assembly was extensively characterized in order to assess its irradiance uniformity and the required driving current for the LED module to provide an optical output similar to that of an 8-W BLB. Initial scans of four UV-A fluorescent black

lights from GE, Eiko, Philips, and Sylvania demonstrated that the GE and Eiko lamps are similar in their spectra and intensity. The Philips lamp ranked the highest in irradiance among the four lamps examined, while the Sylvania lamp had the lowest irradiance and a very broad peak. Hence, the Philips brand lamp was used in this study. Relative to the UV-A LED, the UV-A BLB had a broader peak (354-388 nm) centered at 365 nm and an additional peak at 405 nm that is out of the TiO_2 action spectrum (<388 nm) (Figure 5). The LED spectrum peak was narrower (357-378 nm) and all of the radiation fell within the TiO_2's action spectrum. Furthermore, the spectra of adjacent LED linear arrays (LED Array 1 and Array 2) were identical (Figure 5).

Figure 5 here

Lateral irradiance profile of the LED assembly was measured every 5 mm from the first LED along the lateral axis directly opposite to one of the 4 arrays (angle 0 degree) as well as opposite to the space between two arrays (angle 45 degree) at the forward current of 100 mA. Irradiance from the LED assembly was not less uniform than desired (Figure 6). The lowest intensity was about 55% of the peak intensity, occurring directly between two LEDs in an individual array. The average irradiance (E) at angle 0 degree was 6.02 mW cm^{-2} with 2.49 mW cm^{-2} at angle 45 degree, resulting in a mean of 4.25 mW cm^{-2} for the assembly. The overall mean irradiance for the LED module was 70% of the predicted value (Figure 6b). The discrepancy could be explained by the directionality (120 degree) of the LED radiation and how the light was measured (Figure 3). The combination of the small sensor aperture (12.7 mm) and the close distance (approximately 8 mm) between the sensor and the light source prevented some of the photons from adjacent LEDs from entering the integrating sphere (Figure 3a). As a result, the measured value was underestimated comparing with that obtained in the absence of the attenuation aperture (Figure 3b). Nevertheless, the opacity of STC pellets packed immediately outside of the quartz sleeve in a working PCO reactor would act as the attenuation aperture and prevent the photons outside the radius of 12.7 mm aperture from reaching the catalyst located where the light sensor was placed. We believed that the measured value was a more accurate representation of the light level the catalyst would intercept rather than the predicted value. In contrast, the 8-W UV-A BLB lamp from Philips measured in the same way showed a uniform irradiance of 4.0 ± 0.2 mW cm^{-2} along the both radial and lateral axes.

Figure 6 here

Furthermore, the light output of the LED assembly was also measured at I_F between 30 to 500 mA. As with the individual LEDs, the irradiance of the LED assembly was directly proportional to the driving current in the range of 30 to 500 mA ($E = 0.0449I_F - 0.2235$, $R^2 = 0.9999$). Consequently, a nominal 100 mA driving current for the LED assembly delivered the maximal irradiance of an 8-W fluorescent lamp.

Thermal Characteristics of the LED Assembly

LED life span can vary according to environmental and design related factors. Although it is largely determined during the engineering phase of an LED lighting design, overdriving an LED assembly will decrease its life span if thermal management is inadequate. In order to assess the effectiveness of our heat management strategy and to determine the upper limit of driving current (and hence the light output) for the assembly, the temperature of each LED in the assembly was measured at three driving currents (Table 2). The LED temperatures (T_j) were calculated based on the thermal resistance from the LED die to the measuring point being 7 °C W^{-1}. Results showed that a linear relationship between the driving current and measured solder temperature (T_s) or calculated junction temperature (T_j), that is, $T_j = 0.0857I_F + 25.4$ ($R^2 = 0.9999$). From this, the maximal allowable driving current was determined to be 870 mA to operate the LEDs below the manufacturer's recommended maximum Tj of 100 °C. Because the LED used in this study was rated for a maximum forward current 700 mA, the assembly consisting of 12 LEDs electrically strung in two parallel series should allow for a maximum of 1400 mA and result in a light output of 62.6 mW cm^{-2} based on the established relationship between the irradiance and forward current ($E = 0.0449I_F - 0.2235$). It was determined that the LED assembly had a greater light output potential (62.6 mW cm^{-2}) than that the current thermal management strategy could deliver (38.9 mW cm^{-2}). That is, from the thermal perspective, the assembly can only fulfill 62% of its light output potential. This is primarily due to the design constraints for this first generation LED module to be directly comparable with linear fluorescent lamps. Four linear LED arrays were mounted on a small aluminum rod; thermal energy (e.g., 12 W at 500 mA driving current) had to be conducted to the ends for convective dissipation.

Table 2 here

PCO Efficiency of the BLB and LED-irradiated Reactors

The PCO reactor effluent was found to consist of ethanol (VOC contaminant), acetaldehyde (oxidation intermediate), and carbon dioxide (final oxidation product). Acetaldehyde (ACD) was the only quantifiable intermediate in the effluent as indicated by the lack of any other peaks in the GC chromatograms (data not shown). The UV-A BLB-irradiated reactor generated effluent ethanol and acetaldehyde profiles (Figure 7b) similar to those reported for methanol oxidation.[14] Upon the initiation of ethanol-contaminated air flow, effluent ethanol concentration remained very low (2% of the feed) for the first three hours, increased at an accelerated rate between 3 and 10 hrs, and continuously crept upwards even after 10 hrs. This initial lag time for ethanol was attributed to the adsorption of ethanol by STC pellets. In contrast, there was a very short (less than 30 min) or no initial lag time for ACD and CO_2, respectively. The concentration of ACD and CO_2 in the effluent increased steeply upon the addition of feed contaminant, suggesting low and/or no affinity of ACD and CO_2 to the STC. The concentration of CO_2 approached a plateau or a steady state between 5 and 10 hrs, but that of ACD and ethanol reached somewhat steady state only after 10 hr. Therefore, the time period between 10 and 20 hrs was considered as the "pseudo-steady state." The time course profiles of effluent ethanol, ACD, and CO_2 from the UV-A LED reactor (Figure 7a) resembled those of the BLB reactor in general shape, but differed in slope and concentration level at the pseudo-steady state.

Figure 7 and Table 3 here

Mineralization of ethanol in both reactors followed zero-order kinetics and had a rate constant of 19.8 and 28.6 nM CO_2 sec^{-1} for the LED and BLB, respectively. The average concentration of effluent components at this time period was used to assess the PCO efficiency in terms of ethanol removal and mineralization (Table 3). Compared with the UV-A BLB reactor, the LED reactor had a lower effluent ACD and CO_2 but higher EtOH, which translated into lower EtOH removal, mineralization, POC rate and photonic efficiency than the UV-A BLB reactor (Figure 8b through e). The results do not necessarily indicate that the LEDs were a less effective light source, bearing in mind that the LED module's irradiance was not as uniform as the BLB; some of the catalyst was irradiated by less than the average irradiance, which may have accounted for the reduced CO_2 and ACD in the effluent.

The effect of irradiance on PCO efficiency was subsequently examined in the LED reactor. Increasing the irradiance at the catalyst surface reduced effluent ACD and EtOH and increased CO_2 production (Figure 8a). There was a linear relationship between both the mineralization efficiency and rate constant and the irradiance (Figure 8c & d). The influence of increasing irradiance on the percentage of ethanol removal (Figure 8b) was not as pronounced as for the mineralization. This is not surprising and is attributable to the STC's unique property of high physical adsorptivity for polar compounds and photocatalytic activity. However, increasing the irradiance from 4.0 to 17.7 mW cm^{-2} decreased the photonic efficiency (ξ) by 33%. The linear relationship between mineralization and irradiance suggested that an irradiance of 7.6 mW cm^{-2} from the LED module would reach the same mineralization as that of the BLB at its full intensity. In other words, the LED reactor used in this study could achieve the same PCO efficiency for ethanol as an 8-W UV-A FL when it is operated at a forward current (I_F) of 170 mA (i.e., a power input of 3.4 W). These values could be reduced by a more uniform irradiance over the entire surface of the photocatalyst.

Figure 8 here

Power Use Efficiency

Power use efficiency of a light source for PCO encompasses both the electric-irradiant efficiency, or wall plug efficiency (WPE), and the PCO efficiency. WPE (defined as the percentage of irradiant output per electrical input) of the light sources used in this study is shown in Table 4. It is apparent that the WPE of the UV-A LED and UV-A FL were comparable, 17% as the manufacturer specified and 13% as measured in this study. It is interesting to note that the WPE efficiency is higher for longer wavelength LEDs. For example, the same type of LED with spectrum centered at 385 nm has a WPE of 21.6%, representing a 25% increase from that of the 365 nm LEDs. However, it is not known whether the gain in WPE would be offset by the potential loss in PCO efficiency since 385-nm LEDs approach the upper limit of the TiO_2 action spectrum. In terms of PCO efficiency, LEDs in the current design were slightly less efficient when compared to the UV-A FL, but the gap could be closed if a more uniform irradiance over the catalyst is achieved. In addition, PCO efficiency of LEDs could be enhanced by exploitation of its instantaneous "on" and "off" feature for periodic irradiation. It was previously

demonstrated that photonic efficiencies for decomposition of o-cresol by a UV/TiO_2 process in a slurry reactor under controlled periodic illumination of LEDs was higher than that under continuous illumination.[12] As a result, the electric energy required for degradation of the same amount of contaminants decreased significantly by using periodic irradiation.

Table 4 here

CONCLUSIONS

This is the first report of a direct comparison between UV-A LED and UV-A BLB as PCO light sources under similar irradiance. Challenges encountered in achieving uniform LED irradiance over the photocatalyst while maintaining the power use efficiency. Increasing the density of LEDs could no doubt enhance the uniformity of the irradiance, but it would also increase the initial cost of a PCO reactor and the burden of heat management if high-power LEDs are used. The results from our LED reactor suggest that the number of LEDs per unit area may actually be reduced because of the facts that the LED assembly could deliver up to 38.9 mW cm^{-2} and an irradiance of 17.7 mW cm^{-2} resulted in a 97% EtOH removal and an 86% mineralization. It became clear that different design strategies should be considered depending upon the type of UV-A LEDs[15] to be used, for instance, a higher density of low-power LEDs (<10 mW) or high-power LEDs (>100 mW) coupled with light dispersion. Typical approaches for light dispersion in lab-scale reactors include a) coupling LEDs to light transmitting optical fibers coated with a thin film of photocatalysts, and b) using a waveguide through which light travels and emits from sides into surrounding catalysts. Although these approaches have the advantage of transferring small area of a LED's illumination to a much greater surface area, each has its own drawbacks. The former has limited applications to thin films of catalysts because of TiO_2's opacity, while the later creates a gradient of irradiance along the waveguide. A balance between side-emitting and transmitting must be struck to achieve uniform side emission intensity over reasonable lengths. We are currently working on screening light conduit materials & LED-light conduit coupling techniques for effective dispersion of high-power LED's radiation.

PCO efficiency in terms of ethanol removal and mineralization was greater in the UV-A BLB reactor than in the UV-A LED reactor at the same average irradiance (4.0 ± 0.2 mW cm^{-2}). Irradiance level and uniformity over the catalyst was found to have a great impact on the PCO efficiency. PCO efficiency increased linearly as the irradiance over the surface of catalyst increased in the range tested (4 – 18 mW cm^{-2}). We estimated that the LED reactor used in this study could achieve the same ethanol mineralization as a 8-W UV-A BLB when it was operated at forward currents (I_F) of 170 mA, which corresponded to a power input of 3.4 W and an irradiant output of 7.6 mW cm^{-2}. These values are expected to be lower as uniform irradiance and/or periodic irradiation are implemented. The results proved that LEDs are a viable photon source both in terms of PCO efficiency and wall plug efficiency. Continuing efforts in the following areas will strengthen this conclusion: 1) improvements in the design of the LED-PCO reactor for a higher fidelity estimate of power use efficiency; 2) investigation of the trade-off between PCO efficiency and electric-irradiant efficiency by using longer wavelength LEDs (e.g. 385 nm instead of 365 nm); 3) using visible light responsive catalysts to take advantage of the higher quantum efficiency of longer wavelength LEDs.

ACKNOWLEDGMENTS

The work was conducted under the auspices of Life Science Support Contract and the first part of a Kennedy Space Center Innovative Partnership Program (IPP) funded project to highlight the partnership with Lighting Science Groups Corporation (LSGC). Authors are extremely grateful to Dr. David Mazyck of the University of Florida for donating the photocatalyst. The authors would like to thank Mr. Lawrence L. Koss for his invaluable assistance with the PCO test bed construction by making customized parts and Opto 22 data logging. We would also like to extend our appreciations to Mr. J. Schellack and Mr. D. Johnson of LSGC for constructing the LED assembly and KSC prototype shop personnel for fabricating the bench scale PCO reactor.

389 **REFERENCES**

390 1. Hoffmann, M.R.; Martin, S.T.; Choi, W.; Bahnemannt, D.W. Environmental applications of
391 semiconductor photocatalysis; *Chem. Rev.* **1995**, 95, 69-96.
392 2. Mo, J.; Zhang, Y.; Xu, Q.; Lamson, J.J.; Zhao , R. Photocatalytic purification of volatile
393 organic compounds in indoor air: a literature review; *Atmos. Environ.* **2009**, 43, 2229–2246.
394 3. Hodgson, A. T.; Sullivan, D. P.; Fisk, W. J. Evaluation of ultra-violet photocatalytic
395 oxidation (UVPCO) for indoor air applications: conversion of volatile organic compounds at
396 low part-per-billion concentrations; *Lawrence Berkeley National Laboratory*, **2005**, LBNL-
397 58936.
398 4. Zhao, J.; Yang, X. D. Photocatalytical oxidation for indoor air purification: a literature
399 review; *Build. and Environ.* **2003**, 38, 645-654.
400 5. Tompkins, D. T.; Lawnicki, B. J.; Zeltner, W. A.; Anderson, M. A. Evaluation of
401 photocatalysis for gas-phase air cleaning – Part 1: process, technical and sizing
402 considerations; *ASHRAE Trans.* **2005**, 111(2), 60-84.
403 6. Tompkins, D. T.; Lawnicki, B. J.; Zeltner, W. A.; Anderson, M. A. Evaluation of
404 photocatalysis for gas-phase air cleaning – Part 2: economics and utilization; *ASHRAE Trans.*
405 **2005**, 111 (2), 85-95.
406 7. Kwon, S.; Fanb, M.; Cooper, A.T.; Yang, H. Photocatalytic applications of micro- and nano-
407 TiO_2 in environmental engineering; *Crit. Rev. in Environ. Sci. and Tech.* **2008**, 38(3), 197-
408 226.
409 8. Steele, R.V. The story of a new light source; *Nature Photonics* **2007**. 1, 25-26.
410 9. Chen, D. H.; Ye, X.; Li, K. Oxidation of PCE with a UV LED photocatalytic reactor, *Chem.*
411 *Eng. Technol.* **2005**, 28, 95-97.
412 10. Ciambelli, P.; Sannino, D.; Palma, V.; Vaiano, V.; Mazzei, R. S.; A step forwards in ethanol
413 selective photo-oxidation; *Photochem. Photobiol. Sci.* **2009**, 8(5), 699–704.
414 11. Wang, W. Y.; Ku, Y. Photocatalytic degradation of Reactive Red 22 in aqueous solution by
415 UV-LED radiation; *Water Res.* **2006,** 40, 2249 – 2258.
416 12. Chen, H. W.; Ku, Y.; Irawan, A. Photodecomposition of o-cresol by UV-LED/TiO_2 process
417 with controlled periodic illumination; *Chemosphere* **2007**, 69, 184–190.

13. Stokke, J. M.; Mazyck, D. W. Effect of catalyst support on the photocatalytic destruction of VOCs in a packed-bed reactor; *Proceeding of 37th International Conference on Environmental Systems*, **2007**, SAE paper 2007-01-3138.
14. Stokke, J. M.; Mazyck, D. W. Photocatalytic degradation of methanol using silica-titania pellets: Effect of pore size on mass transfer and reaction kinetics; *Environ. Sci. & Tech.* **2008**, 42(10), 3803-3813.
15. Sandhu, A. The future of ultraviolet LEDs; *Nature Photonics* **2007**, 1, 38.

About the Authors

Lanfang H. Levine and Jeffrey T. Richards are senior research chemists with Dynamac Corporation at Kennedy Space Center, FL 32899. Robert Soler and Fred Maxik are both electrical engineers and serve as director of electrical engineering and chief scientific officer, respectively for Research and Development of Lighting Science Group Corporation at 1227 S. Patrick Dr. Satellite Beach, FL 32937. Janelle Coutts is a graduate student from the University of Central Florida and currently a chemistry intern with Dynamac Corporation at Kennedy Space Center. Raymond M. Wheeler is a plant scientist with NASA at Kennedy Space Center, FL 32899. Please address correspondence to Lanfang H. Levine, Space Life Sciences Laboratories, Mail Code: DYN-3; Kennedy Space Center, FL 32899, USA; phone: 321-861-2931; e-mail: lanfang.h.levine@nasa.gov.

TABLES

Table 1. Comparison of test reactors

	Reactor used in Stokke and Mazyck[13]	**Annular reactor in this study**
Reactor Housing ID (mm)	41.4	38.1
Quartz Sleeve OD (mm)	25.4	28.0
Annulus Space (mm)	8.0	5.05
Catalyst Bed Height (mm)	35.8, 71.5, 107.3	60
Bed Volume (cm^3)	30, 60, 90	31.44
Temperature	Not controlled	Controlled to 25 °C

441

442

443 **Table 2.** LED solder temperature (T_s) and dice temperature (T_j) as a function of I_F

I_F (mA) for the LED Assembly	Measured T_s (°C)	Predicted T_j (°C)
100	32.7±0.2	33.9
300	47.8±0.6	51.3
500	62.3±1.0	68.1

444

445 **Table 3.** Effluent composition and PCO efficiency at pseudo-steady state from the BLB and
446 LED reactors at the same irradiance. Values represent the mean (± s.e.) between 10 and 20 hrs.
447 Influent ethanol concentration was 51 ± 0.3 ppm_v.

	UV-A BLB	UV-A LED
Average E, mW cm^{-2}	4.0 ± 0.2	4.0 ± 0.2
Effluent EtOH, ppm_v	4.6 ± 0.6	10.5 ± 0.2
Effluent ACD, ppm_v	18.7 ± 0.3	14.2 ± 0.4
Effluent CO_2, ppm_v	45.5 ± 2.5	28.8
EtOH Removal (%)	91.0 ± 1.3	80.0 ± 0.4
Mineralization (%)	44.3 ± 2.7	28.2

448

449 **Table 4.** Wall plug efficiency (WPE) of the light sources

	UV-A BLB	UV-A LED (Individual)	UV-A LED (Assembly)
Model/Type	F8T5	Nichia NCSU033B	Custom Designed
Electric Input (W)	8.0	1.9	2.0
Optical Output (W) Specified	1.41	0.33	
WPE (%) Specified	17.6	17.1	
Optical Output (W) Measured	1.06		0.26
WPE (%) Measured	13.2		13.0

450

451

FIGURE CAPTIONS

Figure 1. Effect of LED spacing and distance away from the LED (i.e. ½ ∅) on: (a) lateral irradiance uniformity and (b) radial irradiation uniformity.

Figure 2. A 3-D model of the annular reactor shown with the LED light source.

Figure 3. Schematic of the setup for light source characterization, illustrating the effect of aperture size on the amount of photons from the adjacent LEDs entering the integrating sphere.

Figure 4. Schematic of a bench-scale PCO test bed where the objects are not to scale.

Figure 5. Spectra of UV-A LEDs and fluorescent black lights.

Figure 6. Irradiance profiles of the LED assembly determined at I_F=100 mA: (a) lateral and radial profiles on the outer surface of the quartz sleeve (OD 28 mm) where the photocatalyst is located; (b) comparison between measured average and model-predicted irradiance.

Figure 7. Time-course of the effluent composition during STC-catalyzed oxidation of ethanol in the (a) UV-A LED and (b) UV-A BLB reactors at the same irradiance of 4 mW cm^{-2}. CO_2 concentration was recorded every minute and appears to be affected by the sample stream valve position giving two parallel trend lines.

Figure 8. Effect of the average irradiance over the catalyst surface on STC-catalyzed PCO in the LED reactor: (a) reactor effluent composition at the pseudo-steady state, PCO efficiency in terms of (b) ethanol removal, (c) ethanol mineralization, and (d) PCO rate constant, and (e) photonic efficiency.

FIGURES

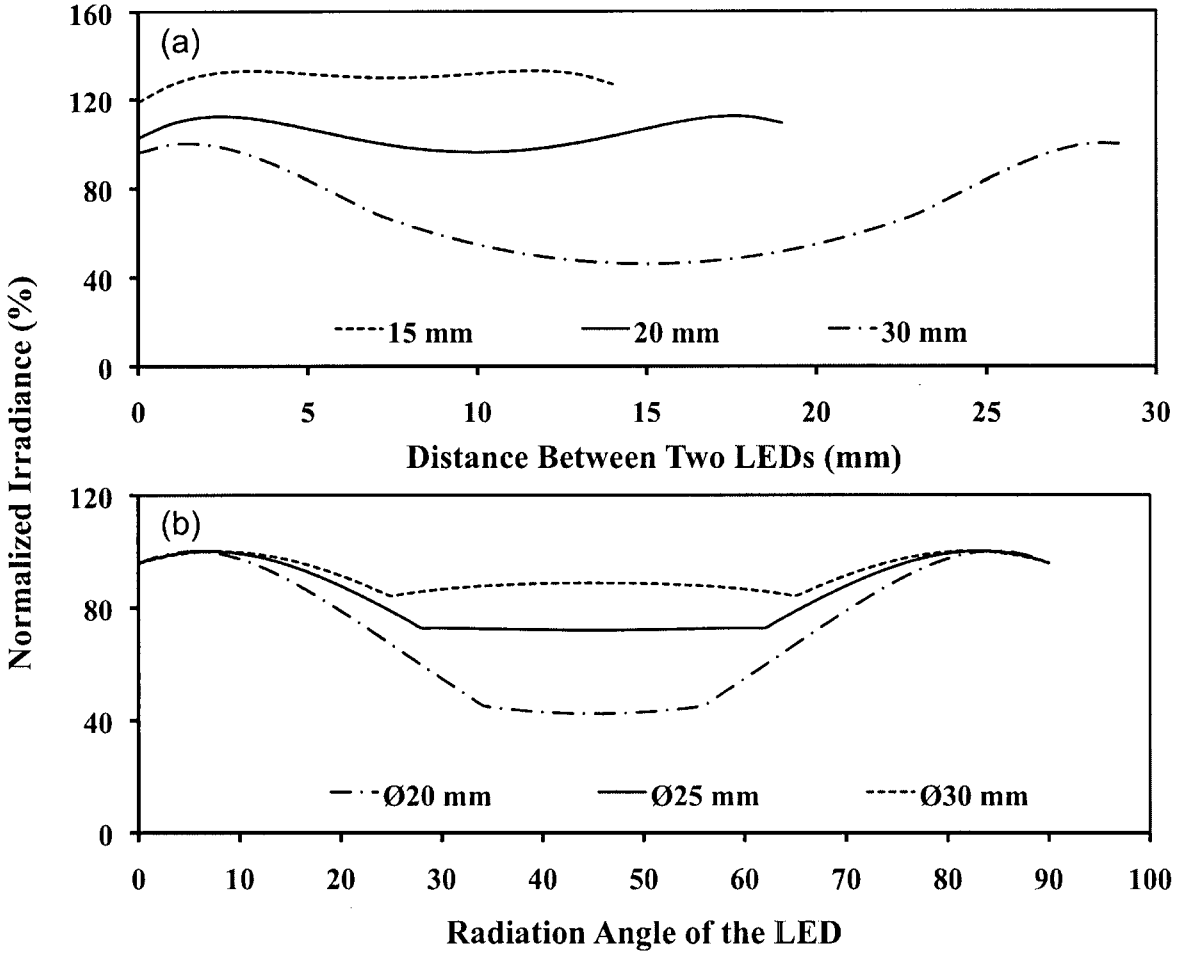

Figure 1. Effect of LED spacing and distance away from the LED (i.e. ½ ∅) on: (a) lateral irradiance uniformity and (b) radial irradiation uniformity.

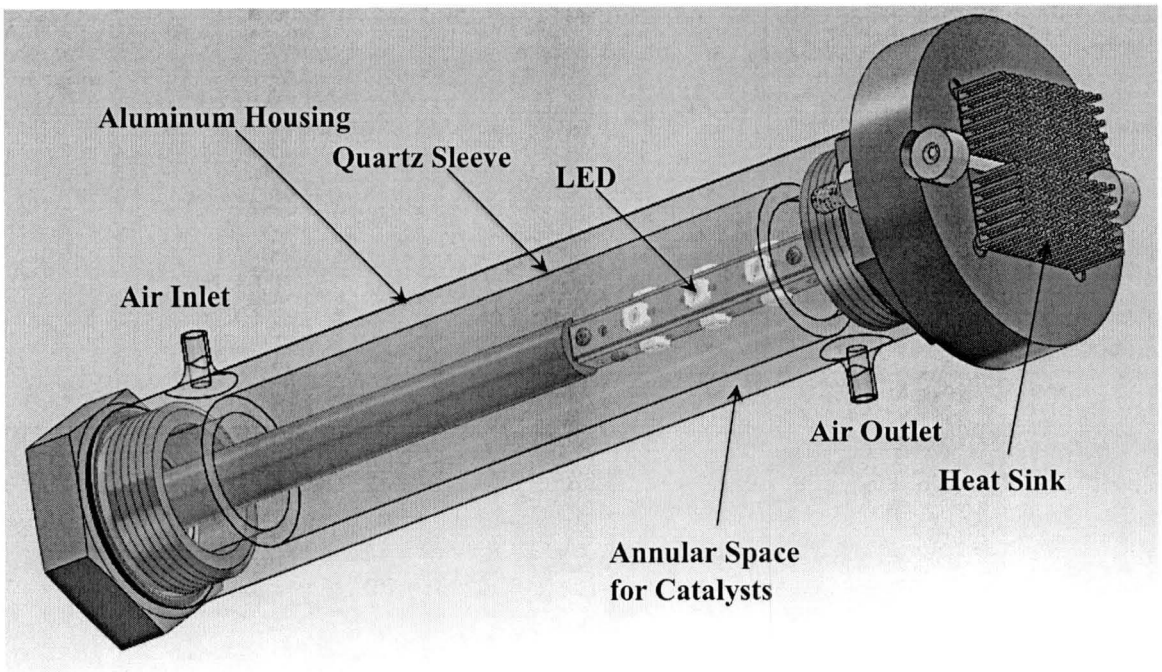

489
490

491 **Figure 2**. A 3-D model of the annular reactor shown with the LED light source.

492

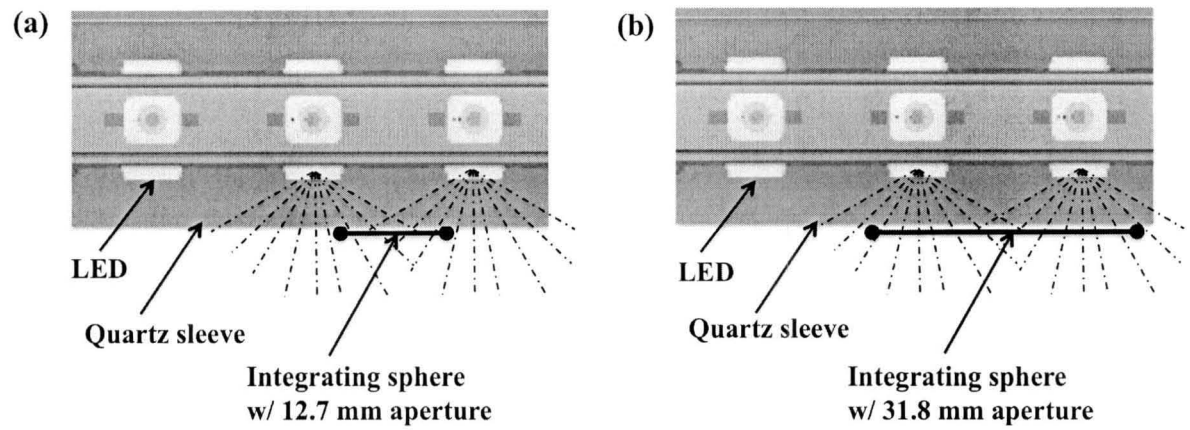

493
494

495 **Figure 3**. Schematic of the setup for light source characterization, illustrating the effect of
496 aperture size on the amount of photons from the adjacent LEDs entering the integrating sphere.

497

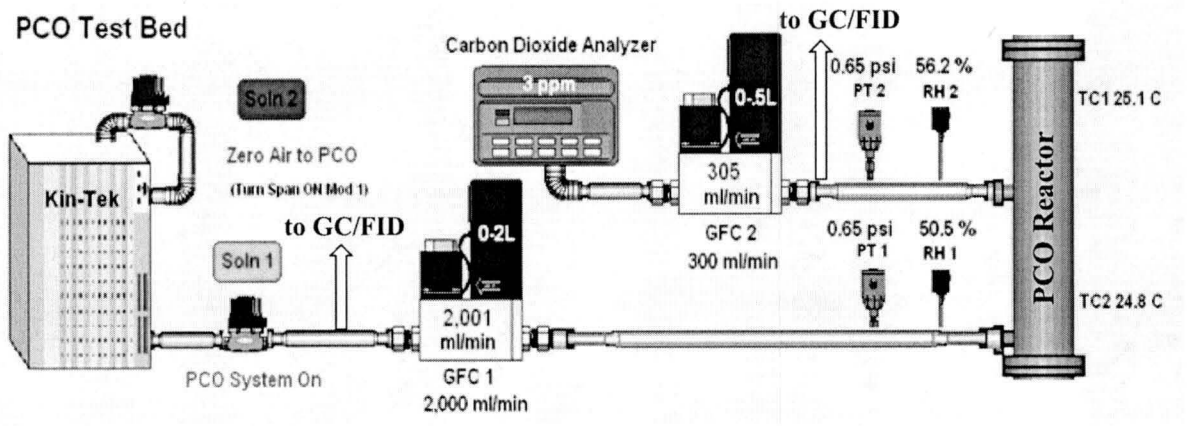

498

499 **Figure 4.** Schematic of a bench-scale PCO test bed where the objects are not to scale.

500

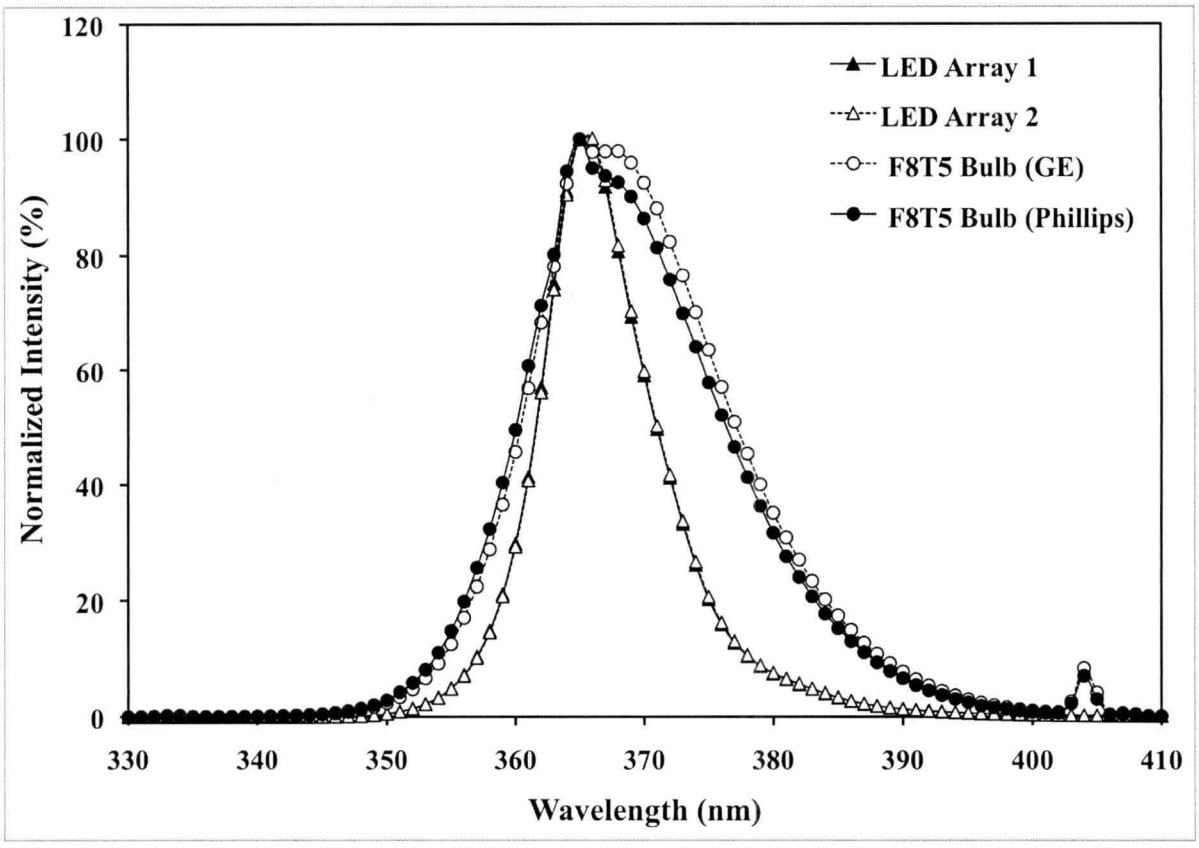

501

502

503 **Figure 5**. Spectra of UV-A LEDs and fluorescent black lights.

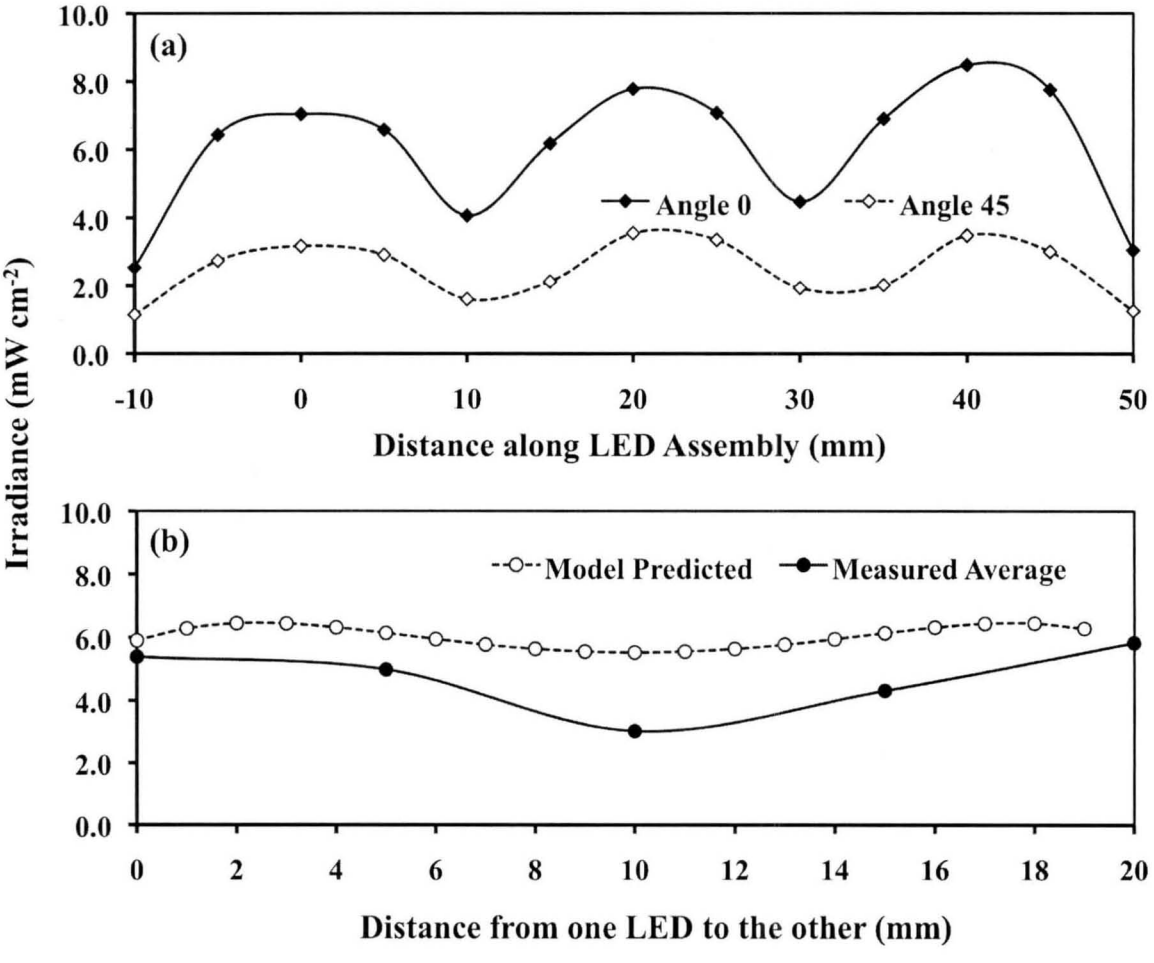

504

505

506 **Figure 6**. Irradiance profiles of the LED assembly determined at I_F=100 mA: (a) lateral and
507 radial profiles on the outer surface of the quartz sleeve (OD 28 mm) where the photocatalyst is
508 located; (b) comparison between measured average and model-predicted irradiance.

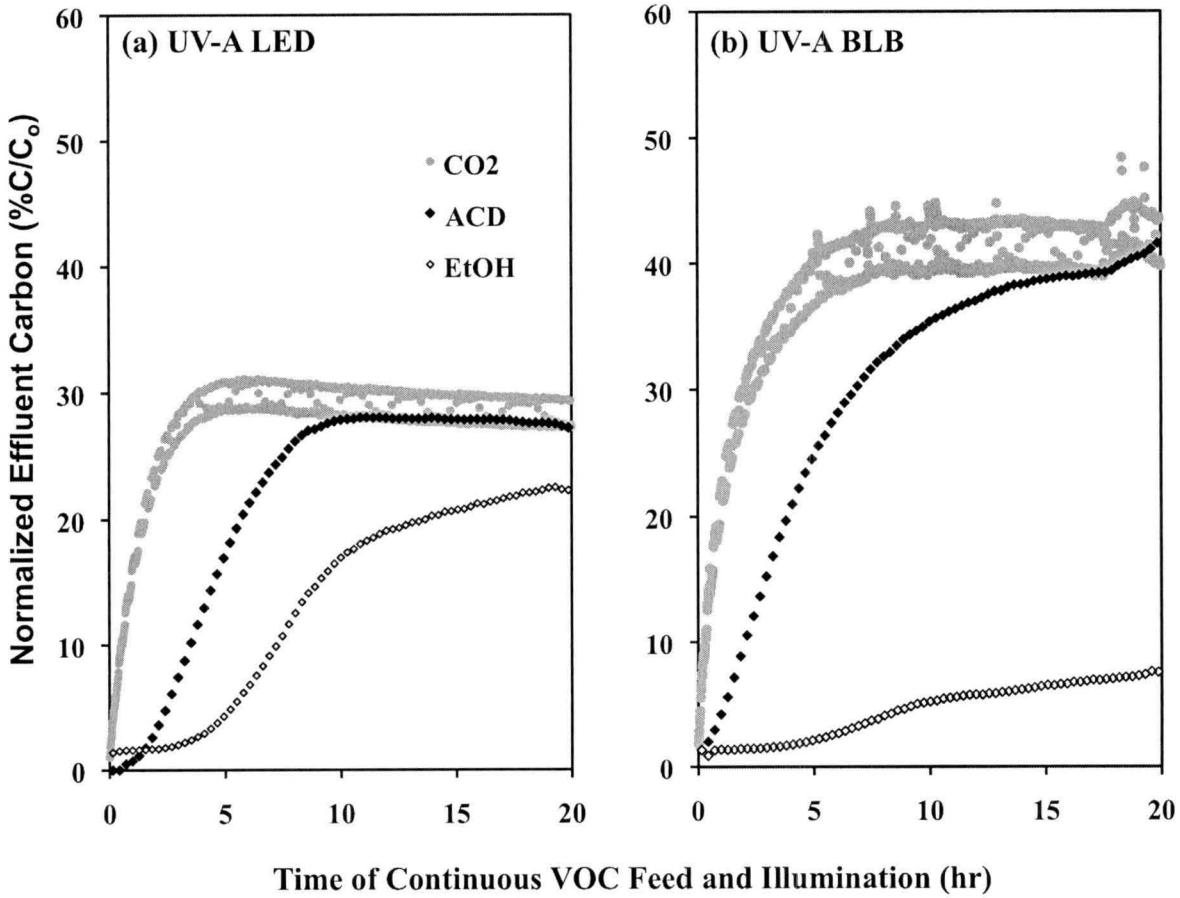

509

510

511 **Figure 7**. Time-course of the effluent composition during STC-catalyzed oxidation of ethanol
512 in the (a) UV-A LED and (b) UV-A BLB reactors at the same irradiance of 4 mW cm^{-2}. CO_2
513 concentration was recorded every minute and appears to be affected by the sample stream valve
514 position giving two parallel trend lines.

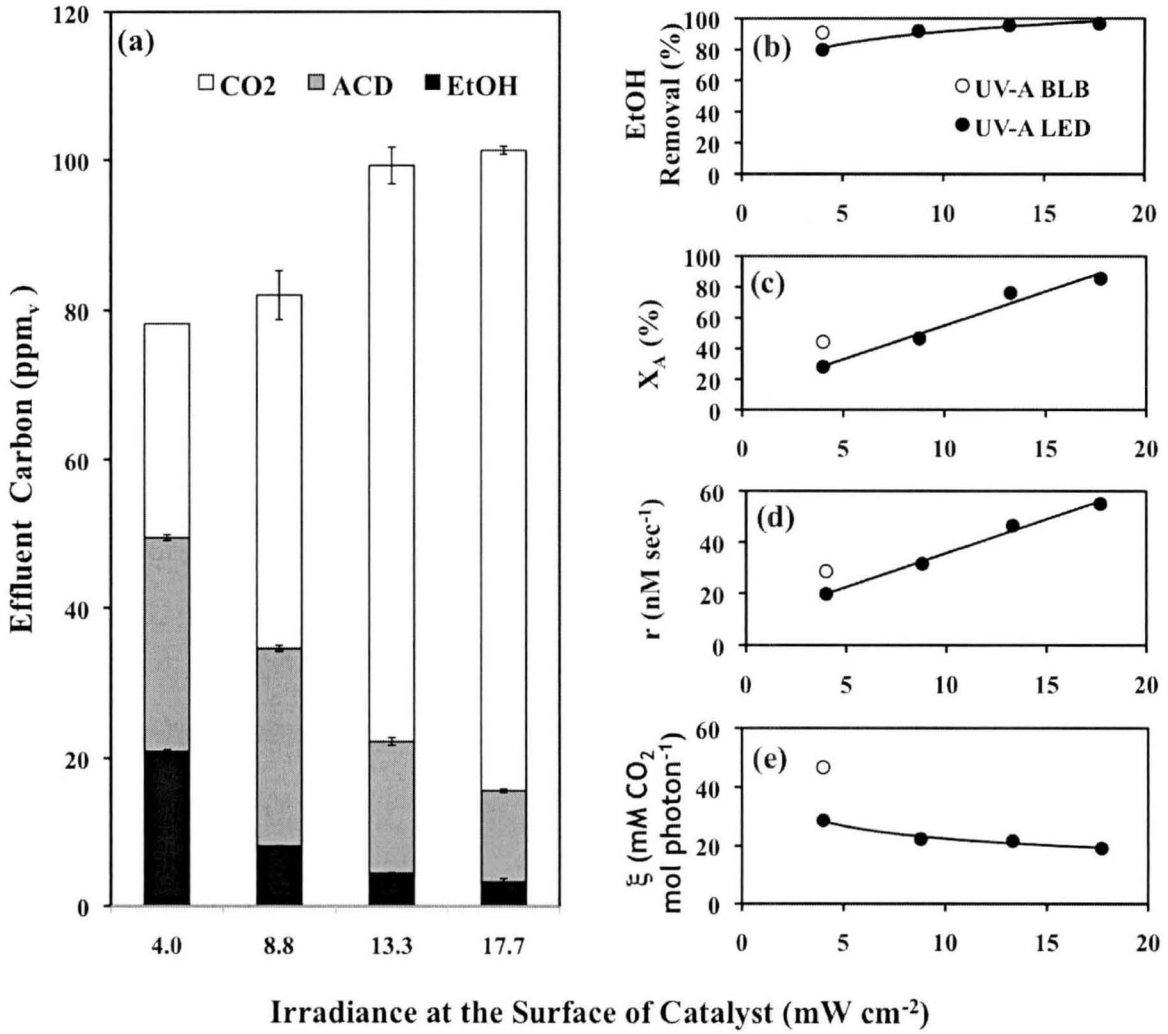

515

516

517 **Figure 8**. Effect of the average irradiance over the catalyst surface on STC-catalyzed PCO in
518 the LED reactor: (a) reactor effluent composition at the pseudo-steady state, PCO efficiency in
519 terms of (b) ethanol removal, (c) ethanol mineralization, and (d) PCO rate constant, and (e)
520 photonic efficiency.